Dislocation Characteristics in Lath Martensitic Steel by Neutron Diffraction

2016 J. Phys.: Conf. Ser. 746 012046

(http://iopscience.iop.org/1742-6596/746/1/012046)

Dislocation Characteristics in Lath Martensitic Steel by Neutron Diffraction

S Harjo[*,,1], T Kawasaki[*], W Gong[*] and K Aizawa[*]**
[*] J-PARC Center, Japan Atomic Energy Agency, Tokai-mura, Naka-gun, Ibaraki 319-1195, Japan
[**] Elements Strategy Initiative for Structural Materials, Kyoto University, Yoshida-honmachi, Sakyo-ku, Kyoto 606-8501, Japan

E-mail: stefanus.harjo@j-parc.jp

Abstract. In situ neutron diffraction during tensile deformation of an as-quenched lath martensitic 22SiMn2TiB steel, was performed using a high resolution and high intensity time-of-flight neutron diffractometer. The characterizations of dislocations were analyzed using the classical Williamson-Hall (cWH) and modified Williamson-Hall (mWH) plots on the breadth method, and the convolutional multiple whole profile (CMWP) fitting method. As results, the dislocation density as high as 10^{15} m^{-2} in the as-quenched martensitic steel was determined. The dislocation density was found to decrease qualitatively with plastic deformation by the cWH and mWH plots, but hardly to change by the CMWP method. The scanning transmission electron microscopy observation supported the results of the latter method. In the CMWP method, the parameter *M* that represents the arrangement of dislocations was found to decrease rapidly where a very high work hardening was observed.

1. Introduction

The as-quenched lath martensitic steel is one important structural material because it consists fine structures and high dislocation densities showing high strengths. The lath martensitic steel exhibits extremely low elastic limit [1], indicating that the work hardening after the yielding at the beginning of plastic deformation is very high. To understand the deformation behavior, the changes in dislocation density in lath martensitic Fe-18Ni alloys with cold rolling and tensile deformation have been measured using the X-ray [1] and neutron diffractions [2] by employing the classical Williamson-Hall (cWH) plot [3]. The dislocation density was determined to decrease with plastic deformation, though a very high work hardening was observed at the beginning of tensile deformation.

Dislocation density has been evaluated mainly using two primary methods, transmission electron microscopy (TEM) [4] and X-ray diffraction (XRD) peak broadening defined by the breadth method [5,6]. These techniques have been considered to be mutually complementary. The XRD line broadening analysis yields average statistic data and supports the TEM results [7]. Takebayashi et al. [7] have claimed that the dislocation density determined by the cWH plot is not appropriate estimating larger dislocation density values, because the dislocation contrast factor is not considered. Hence, the modified Williamson-Hall plot (mWH) [5,8] coupled with the modified Warren-Averbach method [5,8] taking the contrast factor into account has recently been used to characterize the dislocation density, character and arrangement [7,9]. However, we believe that these analyses are not satisfactory

[1] To whom any correspondence should be addressed.

because the results obtained from thin films (TEM) or surface layers (XRD) are frequently suspected to be smaller than the average values of a bulky whole specimen. Recently, in situ neutron diffraction has been demonstrated to be a powerful tool in various engineering applications [2,10-12], including thermo-mechanically controlled processing [12].

Hence, in the present study, the deformation behavior of a lath martensitic 22SiMn2TiB steel, was investigated using in situ neutron diffraction during tensile test. The characterizations of dislocation were performed using the WH plots and a convolutional multi whole profile fitting (CMWP) method developed by Ungár and his coworkers [13,14], and the obtained results were compared from each other.

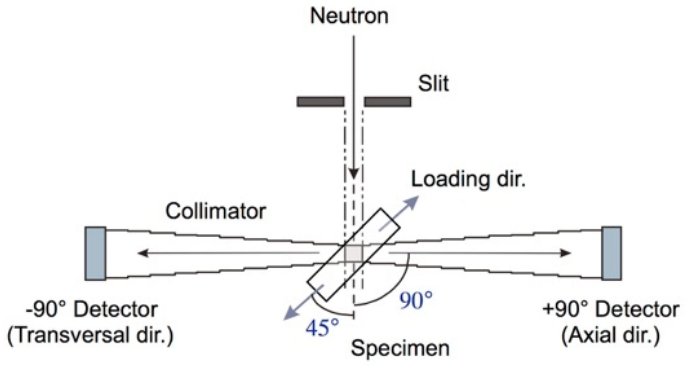

Figure 1. Experimental arrangement of in situ neutron diffraction during tensile deformation on TAKUMI at the MLF of J-PARC.

2. Experimental procedures

The as-quenched lath martensitic steel, 22SiMn2TiB steel [15], was used in this study. The averaged packet and block sizes were 19.6 μm and 3.9 μm, respectively. The rod shape specimen with diameter of 5.0 mm and active length of 30 mm was prepared after the austenitic solution treatment for the in situ neutron diffraction experiment during tensile test. The specimen was mounted horizontally in the loading machine sitting on the sample stage of TAKUMI [16], a high resolution and high intensity time-of-flight (TOF) neutron diffractometer for engineering sciences at Materials and Life Science Facility (MLF) of Japan Proton Accelerator Research Complex (J-PARC). The schematic drawing of experimental setup is shown in figure 1. The neutron diffraction patterns in the axial and transversal directions were measured simultaneously using two detector banks that have the scattering angles of ± 90°. The gauge volume was restricted to be $5.0 \times 5.0 \times 5.0$ mm^3 using the incident beam slit and radial collimators. The TAKUMI instrumental resolution used in this study was tuned to have the instrumental peak resolution of about 0.3 %.

The tensile deformation for in situ neutron diffraction was performed in a stepwise manner. The deformations in the plastic region were increased step by step to arbitrary strains followed by unloading. The neutron diffraction data collection was conducted continuously using an event-recording mode [17] during the tensile deformation. Diffraction patterns related to the unloaded states after plastic deformations were then sliced according to the stress and strain data. The characterizations of dislocation were performed using the WH plots and the CMWP fitting. Diffraction peak profiles of LaB_6 powder measured at the same condition with the in situ neutron diffraction measurement were used to determine the instrumental peak profiles for the dislocation analyses.

The Rietveld refinements on the diffraction patterns were performed using the Z-Rietveld software [18] prior to the dislocation characterization. The specimen contained the retained austenite, and its fraction was determined to be about 3.7 %. The existence of retained austenite was difficult to confirm on the SEM or TEM image, probably due to the tiny size. The lattice constants of martensite and austenite were determined to be 0.28646(0) nm and 0.35912(3) nm, respectively. The austenite peaks still existed after 4.7 % deformation. The inverse pole figures were also determined from the ratios of

integrated intensities of (hkl) peaks. The specimen had random orientation before deformation, and a very weak -fiber texture was developed after 4.7 % deformation.

3. Results and discussion

3.1. Stress-strain curve

Figure 2 shows the stress-strain curve obtained during the tensile deformation for the in situ neutron diffraction. The specimen shows a very high tensile strength of about 1.65 GPa. This steel showed a uniform strain of about 6.1 % and fractured at the strain value of about 14 %, when it was tensioned continuously. The tensile deformation shown in figure 2 includes plastic deformation though the highest strain is 4.7 %. The elastic limit measured from the continuous tension test was about 500 MPa, and therefore the rate of work hardening is extremely high.

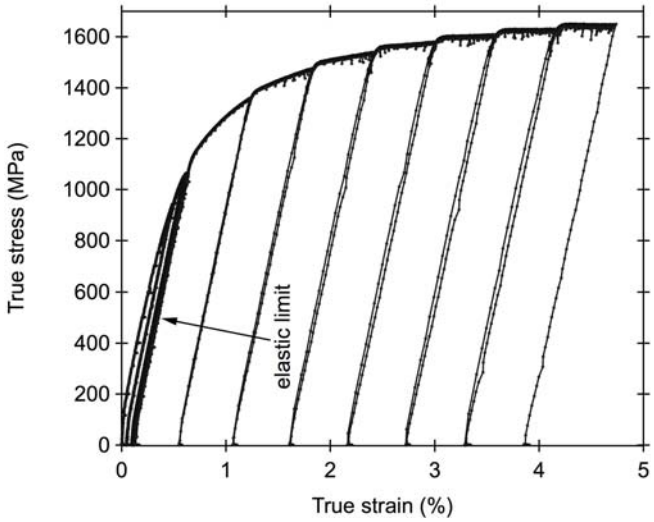

Figure 2. Stress-strain curve of the lath martensitic 22SiMn2TiB steel obtained from the tensile test.

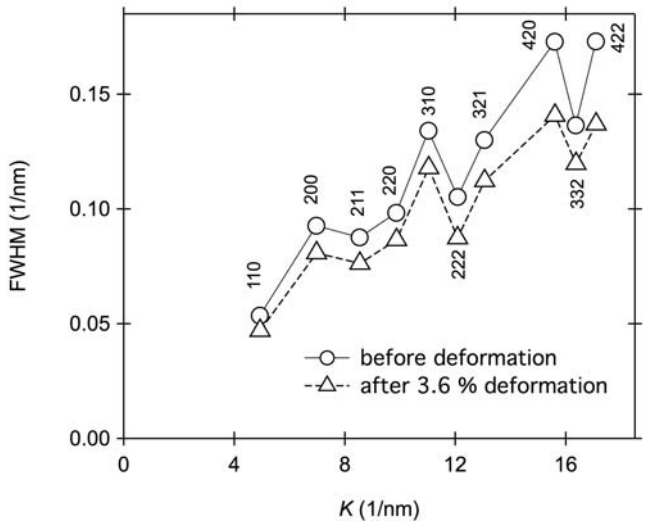

Figure 3. Typical cWH plots obtained for the axial direction before deformation and after 3.6% deformation ($K = 1/d$, where d is the lattice spacing).

3.2. Williamson-Hall plots

The dislocation density is often evaluated from diffraction profiles simply using the cWH plot [3]. Figure 3 shows typical cWH plots for the axial direction. The full width at half maximum (FWHM) data of the specimen is the convolution of the instrumental and physical effects, which are difficult to be separated in physical theories. The scatters of FWHM data of the specimen are large in the cWH plots as shown in figure 3, though the instrumental FWHM data measured using LaB_6 powder was in a good linearity. The dislocation density is estimated from the slope in the cWH plot, and the scatter therefore will decrease the accuracy. The slope of cWH plot for the specimen after 3.6 % deformation is smaller than that before deformation.

Figure 4 shows typical mWH plots for the axial direction at different conditions of deformation. The scatters of FWHM data of the specimen are much improved by introducing the contrast factor (C). However, the trends are still similar with those in figure 3. The slope before deformation is the largest, and it becomes smaller with the increase of strain. These trends speculate qualitatively that the high dislocation density induced during martensitic transformation decrease with the increase of strain. The same tendencies have also been reported in the previous studies for Fe-18Ni alloys [1,2] that employed the cWH plot. According to the Taylor equation [19], shown in equation (1), the work hardening can be described by the increase of dislocation density.

$$\Delta\sigma = \alpha b M_T G \sqrt{\rho} \tag{1}$$

Here, $\Delta\sigma$, α, b, M_T, G, and ρ are the amount of hardening, coefficient α, Burger's vector (constant), Taylor factor (constant), modulus of rigidity (constant), and dislocation density, respectively. Thus, the trends in figures 3 and 4 are difficult to understand the origin of the high rate of work hardening shown in figure 2. Note, that the profile does have the FWHM value and the tail. The tails are ignored in the FWHM values. This is one of the reasons why in any breadth method it fails for providing dislocation densities.

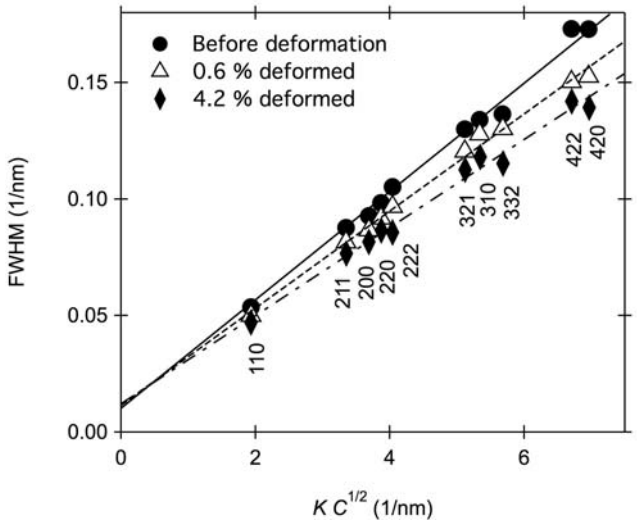

Figure 4. Typical mWH plots obtained for the axial direction at different conditions of deformation (K = 1/d, where d is the lattice spacing).

3.3. • CMWP fitting

The CMWP method is an analysis method to characterize defects from the diffraction profiles based on the modified Williamson-Hall plot combining with a convolutional profile fitting method [13,14].

Figure 5 shows the observed and CMWP-fitted neutron diffraction profiles before deformation. In the CMWP fitting, the second phase of the retained austenite was also analyzed to exclude its influence on the results of the main phase of martensite. All martensite peaks are indexed and some of

the austenite peaks are also indexed. In the first part of the pattern, the 111 austenite peak can be seen as a shoulder of 110 martensite peak.

The parameters obtained by the CMWP fitting for the axial direction are summarized in figure 5. The value of ρ before deformation is already very high of about 4.0×10^{15} m^{-2}. This value is believed to be consistent with that reported in a lath martensitic steel with similar carbon content (0.18 mass %) studied by Morito et al using TEM [4], by considering that the neutron diffraction observes as bulky whole information while the TEM a limited area of thin film. The value of ρ gradually increases with the large increase of strain though the increase of flow stress is observed. The dislocation densities were also clarified using scanning transmission electron microscopy (STEM) observations on three annular dark field images with the incident beam parallel to <111> and two images <001>. As results, the dislocation density before deformation was averagely determined to be 1.17×10^{15} m^{-2}, and that after 4.7 % deformation to be 1.18×10^{15} m^{-2}, showing no significant different between the two conditions. These results confirm the CMWP fitting results that the increase of dislocation density during deformation is small.

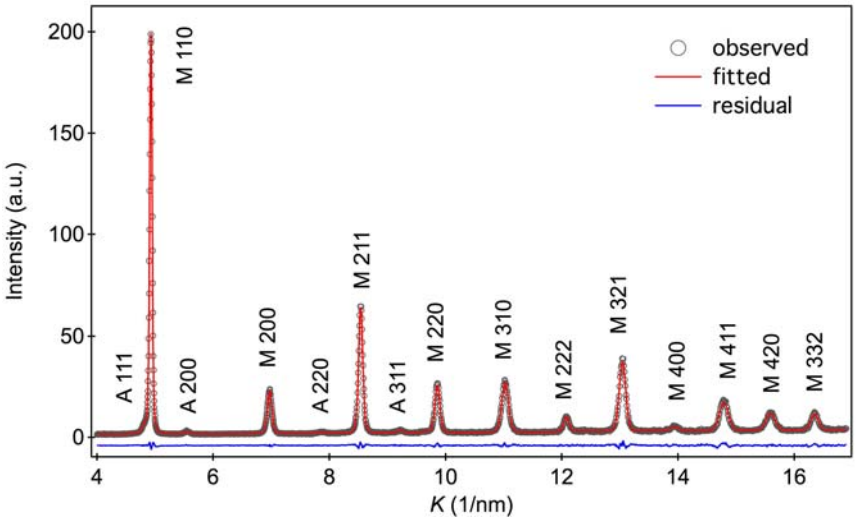

Figure 5. The observed (black-circle symbol) and CMWP-fitted (red line) neutron diffraction profiles before deformation. Blue line is the residual between the fitted and observed profiles.

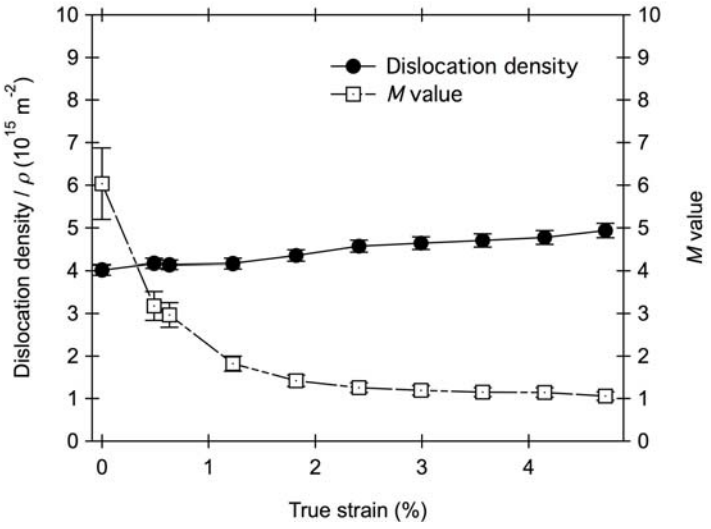

Figure 6. Parameters obtained from the CMWP fitting in the 22SiMn2TiB steel for the axial direction.

The value of contrast parameter q before deformation was determined to be about 1.7, and it was found hardly to change during deformation. The parameter q displays the dislocation character, i.e., the edge or screw component. According to a theoretical computation for iron with slip system of <111>{110}, the value of 1.3 stands for the edge and 2.6 for screw dislocations [20]. The value of q of about 1.7 indicates that the dislocations are mixed with the edge and screw characters. The area-averaged crystallite size was about 57 nm which may display the lath size.

Another parameter M [13], which is a product of the effective cut-off radius of dislocations Re and the square root of ρ ($M = Re\ \rho^{0.5}$ [13]), displays the dislocation arrangement. The value of $M > 1$ stands for random dislocation arrangement, and $M < 1$ for highly correlated arrangement. As is shown in figure 6, the value of parameter M is found to decrease rapidly at the beginning of plastic deformation, then gradually varied with the progress of deformation finally becoming close to 1. This indicates that randomly distributed dislocations in the as-quenched martensite are arranged toward correlated arrangements. Since the increase of dislocation density in the specimen is small during deformation applied in this study, the observed high work hardening is predicted as the result of the increase of coefficient α in the Taylor equation. From comparison between the results in figure 6 and the stress-strain curve in figure 2, the change in parameter M seems to be in inverse proportion to the increase of flow stress. It is speculated that the parameter M has strong relation with the coefficient α in the Taylor equation. However, further discussion to describe the relation is under process.

4. Conclusions

The in situ neutron diffraction during tensile deformation of an as-quenched lath martensitic 22SiMn2TiB steel, was performed using a high resolution and high intensity TOF neutron diffractometer TAKUMI at the MLF of J-PARC. The dislocation density, arrangement and character were analyzed to make clear the work-hardening mechanism of the as-quenched martensitic steel.

(i) The dislocation density in the as-quenched martensitic steel was originally high of 10^{15} m^{-2} order. Although the cWH and mWH plots on the breadth method showed a qualitatively decrease in dislocation density with plastic deformation, the CMWP method revealed little change. The STEM observation supported the results of the latter method.

(ii) According to the results by the CMWP fitting, it is noted that the parameter M related to dislocation arrangement decreases rapidly with plastic deformation keeping little change in dislocation density. The change of parameter M is in the same trend with the change of work-hardening rate.

(iii) The combination of TOF neutron diffraction and CMWP fitting is, therefore, a powerful method to characterize the deformation structures quantitatively using bulky-averaged parameters.

Acknowledgments

Authors wish to acknowledge Prof. Zhengmin Shi for providing the sample for this study, Prof. Yo Tomota, Prof. Tamas Ungar and Prof. Shigeo Sato for valuable discussion. The neutron diffraction experiments were performed at BL19 in Materials and Life Science Facility of J-PARC with the proposals of 2014I0019 and 2014P0102, and got partly financial supports from the Japan Society for the Promotion of Science Grant-in-Aid for Scientific Research (No. 26289264 and 15H05767).

References

[1] Nakashima K, Fujimura Y, Matsubayashi H, Tsuchiyama T and Takaki S 2007 *Tetsu-to-Hagane* **93** 459
[2] Morooka S, Tomota Y and Kamiyama T 2008 *ISIJ Int.* **48** 525
[3] Williamson G K & Smallman R E 1956 *Phil. Mag.* **1** 34
[4] Morito S, Nishikawa J and Maki T 2003 *ISIJ Int.* **43** 1475
[5] Ungár T and Borbély A 1996 *Appl. Phys. Lett.* **69** 3173

[6] Chanda A, De M and Kajiwara S 2000 *Jpn. J. Appl. Phys.* **39** 539
[7] Takebayashi S, Kunieda T, Yoshinaga N, Ushioda K and Ogata S 2010 *ISIJ Int.* **50** 875
[8] Ungár T, Ott S, Sanders P G, Borbély A and Weertman J R 1998 *Acta Mater* **46** 3693
[9] Shintani T and Murata Y 2011 *Acta Mater* **59** 4314
[10] Harjo S, Tomota Y, Lukáš P, Neov D, Vrána M, Mikula P and Ono M 2001 *Acta Mater.* **49** 2471
[11] Tomota Y, Lukáš P, Neov D, Harjo S and Abe Y R 2003 *Acta Mater.* **51** 805
[12] Tomota Y, Xu P G, Oliver E C and Paradowska A 2010 *In-situ Studies with Photons, Neutrons and Electrons Scattering*, ed. T Kannengiesse, S S Babu, Y Komizo and A J Ramirez (Berlin: Springer-Verlag) p 175
[13] Ungár T, Gubicza J, Ribarik G and Borbély A 2001 *J. Appl. Cryst.* **34** 298
[14] Ribárik G, Gubicza J and Ungár T 2004 *Mater. Sci. Eng. A* **387-389** 343
[15] Shi Z, Liu K, Wang M, Shi J, Dong H, Pu J, Chi B, Zhang Y and Jian L 2012 *Met. Mater. Int.* **18** 317
[16] Harjo S, Ito T, Aizawa K, Arima H, Abe J, Moriai A, Iwahashi T and Kamiyama T 2011 *Mater. Sci. Forum* **681** 443
[17] Ito T, Nakatani T, Harjo S, Arima H, Abe J, Aizawa K and Moriai A 2010 *Mater. Sci. Forum* **652** 238
[18] Oishi R, Yonemura M, Nishimaki Y, Torii S, Hoshikawa A, Ishigaki T, Morishima T, Mori K and Kamiyama T 2009 *Nucl. Instrum. Meth. A* **600** 94
[19] Taylor G I 1934 *Proc. R. Soc. A* **145** 362
[20] Ungár T, Dragomir I, Révész A and Borbély A 1999 *J. Appl. Cryst.* **32** 992